International Journal of Modern Engineering Research (IJMER)
www.ijmer.com Vol. 3, Issue. 6, Month. 2013 pp-3493-3499 ISSN: 2249-6645

CFD analysis of double-chambered crematories using biomass producer gas as a fuel source

Yaowateera Achawangkul[1], Naoki Maruyama[1], Chatchawan Chaichana[2]
Masafumi Hirota[1], Akira Nishimura[1], Pimpawat Teeratitayangkul[2]
[1]*Graduate School of Engineering, Mie University, JAPAN*
[2]*Department of Mechanical Engineering, Faculty of Engineering, Chiang Mai University, THAILAND*

ABSTRACT: *This paper describes the simulation results of a biomass producer gas-based, double-chambered crematory using CFD analysis. The specific properties of biomass gas, such as thermal conductivity, specific heat capacity and viscosity, were determined by using the constituents of coffee bean pulp-derived gas obtained from the experiment. The criteria of simulation consist of coffins and human corpses contained in the primary combustion chamber, whereas the standard k-epsilon viscous model and SIMPLE algorithm were used. The simulation results show that the modified model, with a 25 degree downward angle in the primary chamber and an adjusted air nozzle, presents a good effectiveness in heat transfer and turbulent intensity. In addition, the results of the NO prediction present a high formation rate if there is only primary chamber ignition. However, the NO formation rate will increase when operating both primary and secondary chambers. Therefore, using the CFD assistant in the biomass gas-based double-chambered crematory can achieve various benefits, such as reducing apparatus construction costs and the experiment time, including the availability for pollution prediction.*

Keywords: *Biomass, Computational Fluid Dynamics, Crematory, Gasification, Producer Gas*

I. INTRODUCTION

Petroleum fuels such as diesel oil and LPG have been utilized as main fuel sources for cremation, especially in modern crematories that contain a cremation chamber and a flue gas treatment chamber. However, operation costs per cremation become higher due to the increasing of global petroleum prices, which directly affects low income people. In addition, it is necessary to consider the environmental effects of using petroleum fuel. Hence, research and study for alternative energy application must be carried out.

Biomass is one alternative energy resource that presents high potential in Southeast Asian countries. At present, there are several biomass technologies that can be applied for thermal application. Biomass gasification is a thermo-chemical conversion that transforms solid biomasses into a gaseous form (called producer gas or syngas), which can be combusted efficiently. It, therefore, has been introduced for heat generation in many industries. According to the property of biomass producer gas that presents combustion characteristics close to those of liquid petroleum fuel, it is possible to utilize biomass producer gas for the cremation process.

In order to apply biomass producer gas as the main fuel for an actual double-chambered crematory, it is necessary to search for appropriate parameters that perform the highest efficiency in both combustion and emission control. Consequently, computational fluid dynamics (CFD) was used to analyze flow characteristics and significant parameters such as temperature, the turbulent scheme, and a pollution forecast.

Thavornun S. [1] studied and researched energy saving ideas for human crematories using diesel oil as the main fuel source. The primary burner should be located 25^{o} at downward angle on the backside of the primary chamber wall in order to provide maximum impingement of the flame onto the corpse. Concerning fuel consumption, the incinerator uses 35 liters of diesel oil on average throughout the cremation process.

Doungsupa N. [2] studied the simulation of combustion in a ceramic fiber kiln using computational fluid dynamics (CFD). The ceramic fiber kiln contains eight LPG burners with a 1 m^3 effective volume, whereas the CFD model solves conservation equations for mass, momentum and energy with the $k-\varepsilon$ turbulent and non-static running model. The comparison between CFD simulation and actual experiments were that both results showed good agreement for temperatures below $800^{o}C$. In addition, the results also showed that the model with a slowly increasing pressure from 3 to 10 psi and 50% open damper the best condition.

Vorayos N. [3] studied computational fluid dynamics to determine the hot air ($70^{o}C$) velocity flow field in a 2-dimensional model of tobacco curing barn by appointing the velocity of injected hot air as 2.8 m/s with a turbulent model. The solution showed that the low velocity contour usually took place at the middle of furnace, while the high velocity contour occurred between the low velocity contour and the furnace's wall. In addition, it was also found that if the tobacco furnace has a height and length ratio (H/L) less than 0.3, air distribution cannot reach the back of the furnace, which especially affects the quality of tobacco contained towards the back.

II. EQUATIONS

2.1 Governing equations

Fundamental governing equations used for simulation are Navier-Stokes Equations, which consist of mass conservation and momentum conservation.

$$\frac{\partial \rho}{\partial t}+\nabla\cdot\left(\rho\vec{V}\right) = 0 \tag{1}$$

$$\frac{\partial(\rho u)}{\partial t}+\nabla\cdot\left(\rho\vec{V}u\right) = \frac{\partial(-P+\tau_{xx})}{\partial x}+\frac{\partial \tau_{yx}}{\partial y}+\frac{\partial \tau_{zx}}{\partial z}+\rho f_x \tag{2}$$

$$\frac{\partial(\rho v)}{\partial t}+\nabla\cdot\left(\rho\vec{V}v\right) = \frac{\partial \tau_{xy}}{\partial x}+\frac{\partial(-P+\tau_{yy})}{\partial y}+\frac{\partial \tau_{zy}}{\partial z}+\rho f_y \tag{3}$$

$$\frac{\partial(\rho w)}{\partial t}+\nabla\cdot\left(\rho\vec{V}w\right) = \frac{\partial \tau_{xz}}{\partial x}+\frac{\partial \tau_{yz}}{\partial y}+\frac{\partial(-P+\tau_{zz})}{\partial z}+\rho f \tag{4}$$

2.2 Heat transfer model

An energy conservation equation is used for heat transfer inside a control volume prediction.

$$\frac{\partial(\rho h_0)}{\partial t}+\nabla\cdot\left(\rho\vec{\nabla}h_0\right) = \nabla\cdot(k\nabla T)+\frac{\partial p}{\partial t}+\left[\frac{\partial(u\tau_{xx})}{\partial x}+\frac{\partial(u\tau_{yx})}{\partial y}+\frac{\partial(u\tau_{zx})}{\partial z}\right]+\left[\frac{\partial(v\tau_{xy})}{\partial x}+\frac{\partial(v\tau_{yy})}{\partial y}+\frac{\partial(v\tau_{zy})}{\partial z}\right] \tag{5}$$
$$+\left[\frac{\partial(w\tau_{zx})}{\partial x}+\frac{\partial(w\tau_{yz})}{\partial y}+\frac{\partial(w\tau_{zz})}{\partial z}\right]+S_h$$

2.3 Standard $k-\varepsilon$ model

Standard $k-\varepsilon$ models are applied to the proper turbulent model in this research, which are represented in (6)-(7).

$$\frac{\partial}{\partial x_i}(\rho U_i k) = \frac{\partial}{\partial x_i}\left[\frac{\mu_t}{\sigma_k}\frac{\partial k}{\partial x_i}\right]+G-\rho\varepsilon \tag{6}$$

and
$$\frac{\partial}{\partial x_i}(pU_i\varepsilon) = \frac{\partial}{\partial x_i}\left[\frac{\mu_1}{\sigma_\varepsilon}\frac{\partial \varepsilon}{\partial x_i}\right]+C_1\frac{\varepsilon}{k}G-\rho C_2\frac{\varepsilon^2}{k} \tag{7}$$

where G and μ_t are the production rate of turbulence and the turbulence eddy viscosity, respectively.

$$G = \mu_e\left[\left(\frac{\partial u_i}{\partial x_i}+\frac{\partial u_j}{\partial x_j}\right)\frac{\partial u_i}{\partial x_j}\right] \tag{8}$$

$$\mu_t = \frac{\rho C_D k^2}{\varepsilon} \tag{9}$$

The Prandtl/Schmidt number (σ_ε) and model constants (C_1, C_2, C_D, σ_k) are shown in Table 1.

Table 1 Constants used for standard $k-\varepsilon$ model

C_1	C_2	C_D	σ_k	σ_ε
1.44	1.92	0.09	1.00	1.30

2.4 SIMPLE algorithm

The Semi-Implicit Method for the Pressure-Linked Equation (SIMPLE) algorithm is used to solve for the model's velocity flow field [4].

III. PRODUCER GAS PROPERTIES

The constituent of biomass producer gas was obtained from an experiment that used coffee bean pulp as fuel [5]. After that, the significant properties, such as thermal conductivity, viscosity and specific heat capacity, could be determined.

Table 2 Composition of coffee bean pulp producer gas

Constituent	H_2	O_2	N_2	CO	CH_4	CO_2
Content (% by volume)	14.9	6.2	39.7	22.5	2.9	13.8

Table 3 Significant properties of coffee bean pulp producer gas

Specific heat capacity (J/kg-k)	1,467.70
Viscosity (N-s/m^2)	5.81 x 10^{-5}
Thermal conductivity (W/m-k)	0.13745

IV. METHODOLOGIES

4.1 Crematory model implementation

SolidWorks 2012 is used for model implementation. The models of double-chambered crematories are separated into 4 types (A1-A4), as shown in Table 4. Five auxiliary air nozzles are arranged at both the left and right sides of the chamber with different incline angles. On the chamber backside wall is the primary producer gas burner's position, with an incline angle of 0^o for the commercial model (A1). Concerning the modified model (A3 and A4), the primary burner is located at a 25^o downward angle in order to provide maximum impingement of the flame onto the coffin and corpse.

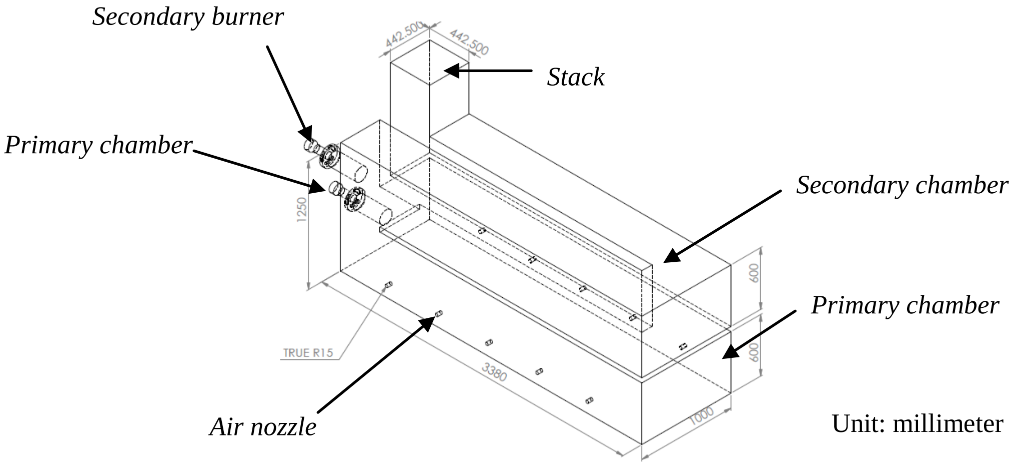

Fig.1 Schematic dimension of crematory

Table 4 Dimension of double-chambered crematory models

Conditions	A1 (Commercial type)	A2	A3	A4
		(Modified model)		
Chamber's dimensions (W x H x L) (mm.)	1,000 x 600 x 3,380			
Primary burner incline angle (deg)	0^o	0^o	25^o	25^o
Secondary burner incline angle (deg)	0^o	0^o	0^o	0^o
Auxiliary air incline angle	0^o	$\phi = 30^o$ $\alpha = 30^o$	0^o	$\phi = 30^o$ $\alpha = 30^o$

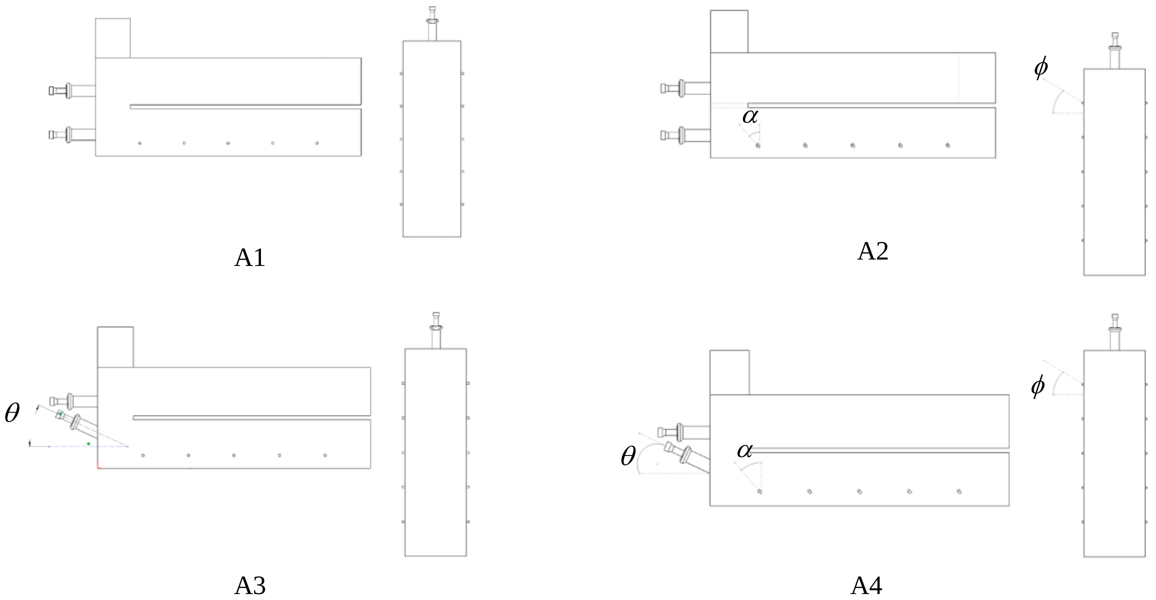

Fig.2 Crematory's model used for simulation

In order for the implemented model to be similar to actual cremation, the coffin model was also implemented. The coffin model was a replicate of the commercial coffin sold in Thailand, with the dimensions of 50 x 50 x 180 cm.

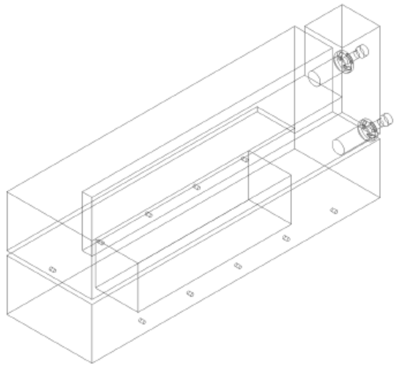

Fig.3 Coffin model implementation in the crematory

4.2 Simulation methodology and initial boundary conditions

ANSYS FLUENT was used to simulate flow characteristics inside the model. A pressure outlet boundary condition was applied to the outlet and the walls were treated at a constant wall temperature or adiabatic wall temperature. The wall was assumed to be stationary with no-slip conditions applied to the wall surface ($\vec{V}_x = \vec{V}_y = \vec{V}_z = 0$).

Velocity of producer gas at 1st burner	5 m/s
Velocity of producer gas at 2nd burner	5 m/s
Velocity of air injected to 1st burner	5.6 m/s
Velocity of air injected to 2nd burner	5.6 m/s
Velocity of auxiliary air injected to primary chamber	20 m/s
Temperature of producer gas	300 K
Temperature of combustion air	300 K

V. RESULTS AND DISCUSSION

5.1 Temperature

From the simulation results, as shown in Fig.4, the maximum temperature reached during the combustion reaction is approximately 1,700 K, which is close to the theoretical flame temperature of biomass producer gas combustion. If the crematory A1 (commercial model) was simulated using the coffin model, the temperature inside the primary chamber would be become highest at the exit of burner. However, the temperature at the front side of the crematory still had the lowest value, equal to that of the ambient temperature. This phenomenon occurred because some of the combustion heat from the burner was drafted into the secondary chamber by the influence of the exhaust fan, and the direction of the auxiliary air injected from the nozzle was dispersed perpendicularly onto the coffin's surface, causing the air flow to counter the combustion heat. Hence, a majority of the heat was smoldered in the backside of the crematory.

When simulating the Model A2 crematory, where the incline angle of the air holds were modified, it was found that the temperature between the coffin and the crematory wall, including the front side, became higher compared to the A1 model simulation. When the airflow from the nozzles hits the coffin's surface, a majority of the air is directed toward the crematory's front, and also forces combustion heat from the back to the front.

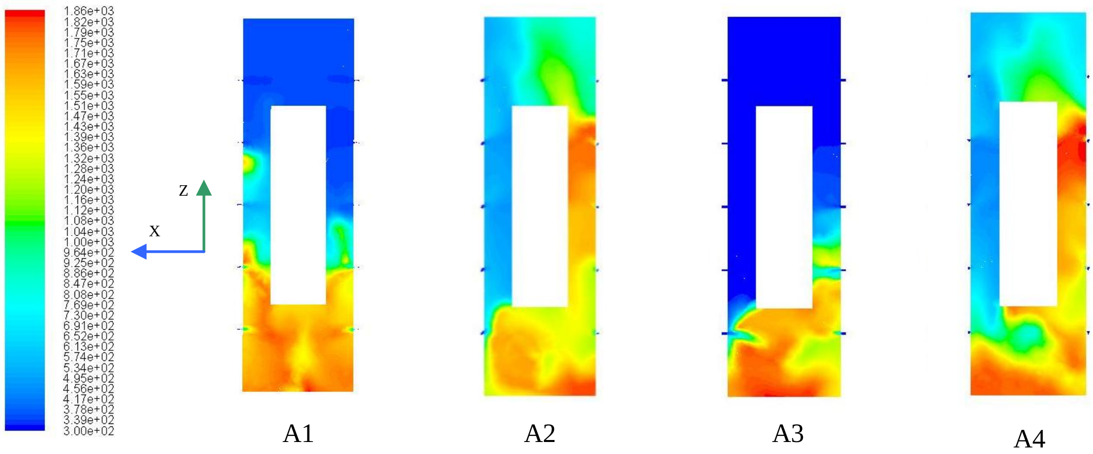

Fig.4 Top view of temperature contours inside the primary chamber with a coffin model

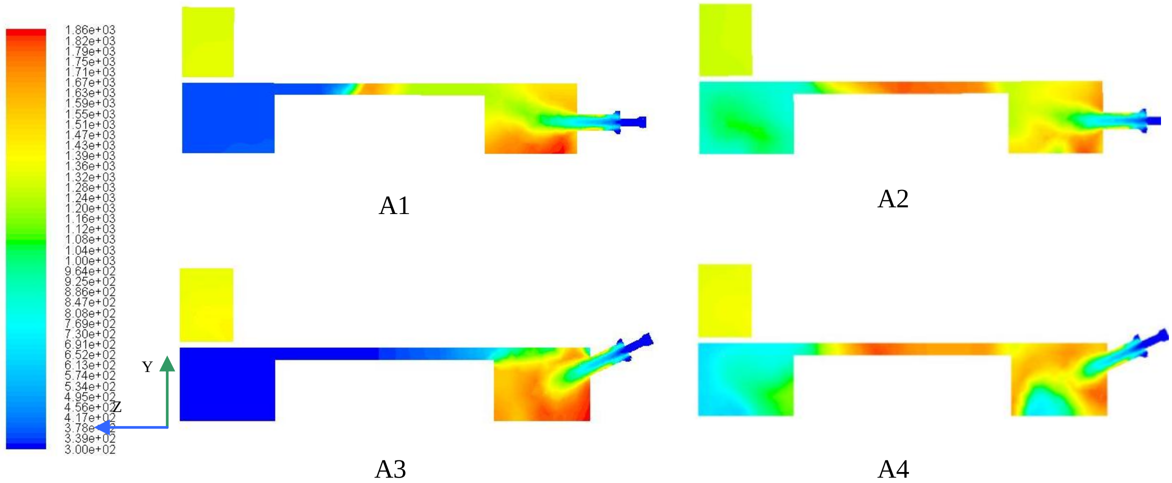

Fig.5 Side view of temperature contours inside the primary chamber with a coffin model

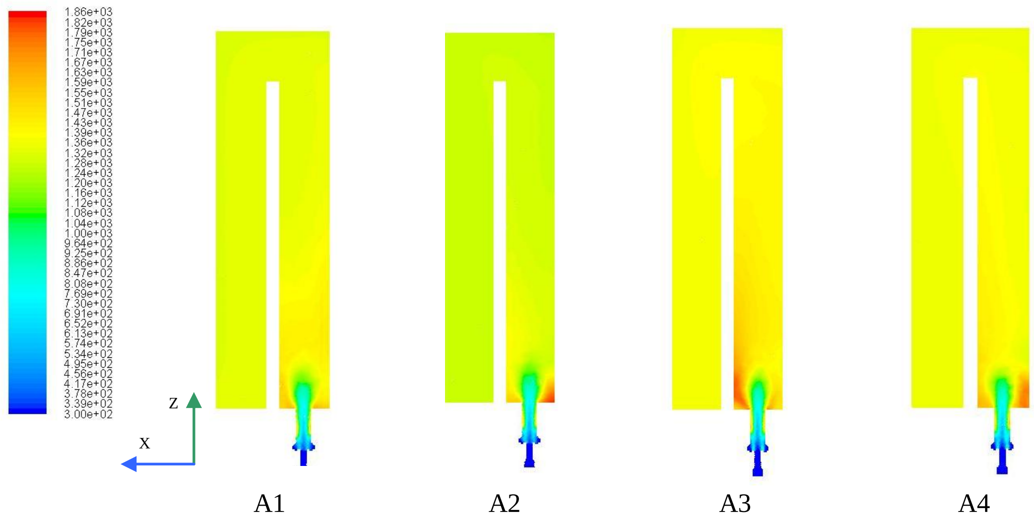

Fig.6 Top view of temperature contours inside the secondary chamber

When simulating the Model A2 crematory, where the incline angle of air holds were modified, it was found that the temperature between the coffin and the crematory wall, including the front side, became higher compared with the A1 model simulation. When the airflow from the nozzles hits the coffin's surface, a majority of the air is directed toward the front of the crematory, and also forces combustion heat from the back to the front.

The simulation of Model A3, in which the burner incline angle was 25^{o} downward, also resulted in worse heat distribution, just as in Model A1. The position that had a high temperature was only in the back of the crematory, while the majority of the crematory model had an ambient temperature at the beginning. Consequently, this model was also deficient for the actual cremation in terms of a great deal of fuel consumption.

Finally, the simulation results of Model A4, in which both the burner and air hold incline angle were modified, presented a good heat distribution. The average temperature beside the coffin was approximately 1,500 K, while the temperature towards the crematory's front was 900 K on average. In addition, because of the little space between coffin's top and the crematory's upper wall, a main obstacle was created against heat transferring throughout the coffin's topside. From the simulations results, as shown in Fig.6, the distribution's contour of combustion heat between the coffin's top and the upper wall of models A2 and A4 was more efficient compared to models A1 and A3.

Accordingly, it can be concluded that the adjusted air hold's angle essentially influenced heat transferring to the front of the crematory . The models in which the burners and air hold angles were modified performed better heat transfers so that the coffin could reach the firing point and ignited faster, which can also reduce the overall cremation time.

5.2 Turbulent intensity

Turbulent intensity is used to investigate the effectiveness of the air flow inside the crematory, including the blending between producer gas and auxiliary air. Figure 7 shows the contour of turbulent intensity inside the primary chamber. It was found that the modified models (A2 and A4), in which the air nozzle angle was adjusted, presented better turbulent intensity compare to the commercial model (A1). This characteristic suggests that the modified models with adjusted air nozzles result in a more effective air and fuel gas blending. At the same time, it can be implied that the combustion reaction in the modified crematory is efficient.

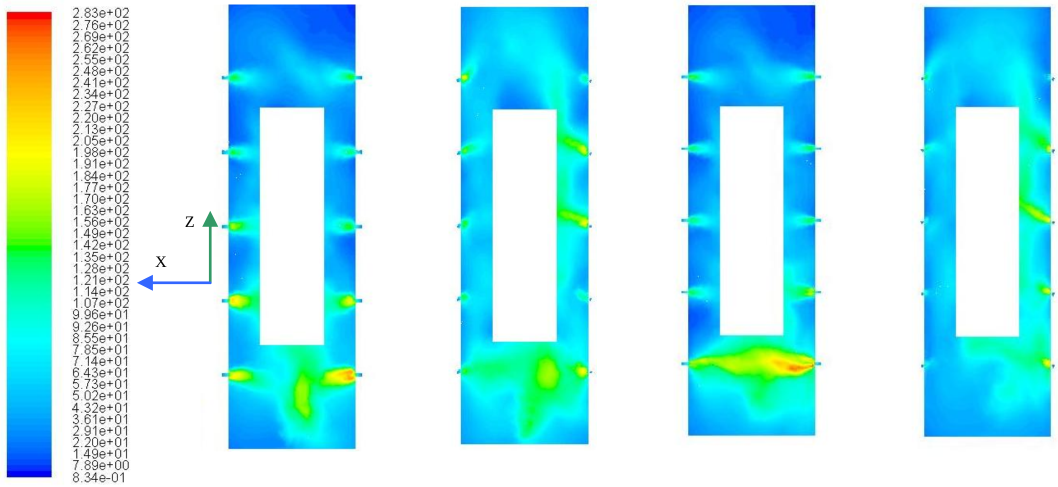

A1 A2 A3 A4

Fig.7 Turbulent intensity (%) contour of the crematory's primary chamber

5.3 NO formation

According to the composition of biomass producer gases that contain a Nitrogen constituent, the occurrence of pollution, such as a formation oxide of Nitrogen (NO_x), is also necessary to be considered. Hence, the prediction of NO formation is explained in this paper.

Figure 8 shows the contour of NO formation inside the crematory model when only the primary burner was operated. It was found that the formation of NO achieved a maximum in the back of the crematory, which was 245,000 mg/m^3. On the other hand, the average amount of NO formation throughout the primary chamber was 123,000 mg/m^3. However, the rate of NO formation decreased in the secondary chamber, and became zero in the crematory's stack. The reduction of NO in the secondary chamber can be explained by the low temperature in the secondary chamber, which then decreased the rate of NO formation, which is dependent on the temperature, until it was equal to zero.

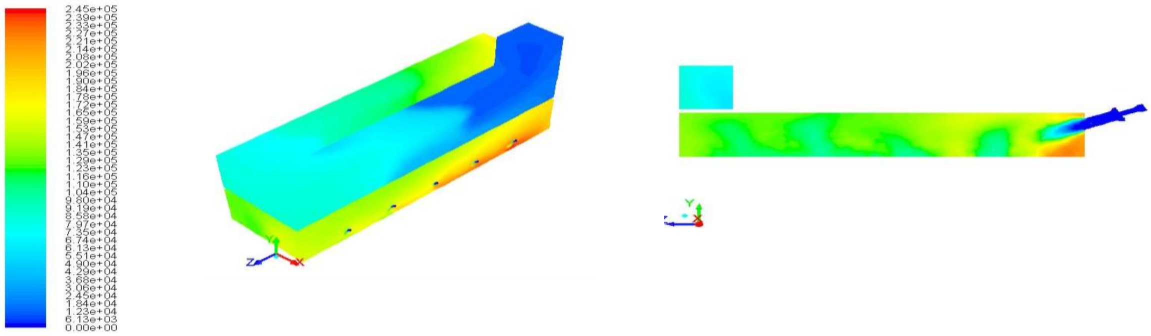

Fig.8 NO formation contour (mg/m^3) if operating only the primary burner

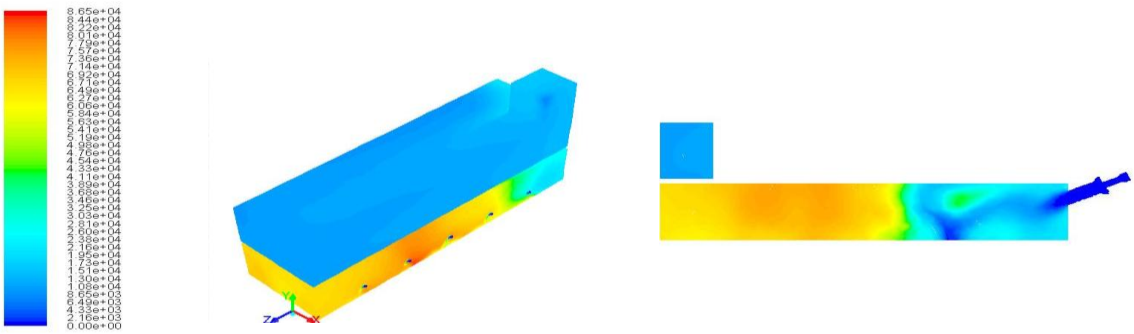

Fig.9 NO formation contour (mg/m^3) if operating both the primary and secondary burners

If both the primary and secondary burners are operated, as shown in Fig.9, the average NO formation inside the primary chamber was approximately 70,000 mg/m^3, and mainly reached its highest in the middle of the crematory. In addition, the NO concentration inside the secondary chamber and in the stack was approximately 20,000 mg/m^3, and then reduces gradually. Finally, the NO formation rate at the crematory's stack becomes 3,000 mg/m^3. Although it is found some NO formation at the stack for this case, compare to the operating only primary burner, however, the NO formation inside the primary chamber is lower than in the operation of only the primary burner. Consequently, NO formation inside the primary chamber can be reduced by operating the secondary burner.

VI. CONCLUSION

Owing to the property of biomass producer gas derived from a gasification process that is different from petroleum fuel, it is essential to pay attention to any application in which the producer gas is used. In particular, cremations that have high temperatures and efficient pollution control are needed. The CFD analysis, therefore, carries an advantage in reducing apparatus preparation costs and the time it takes to experiment. The analysis results show that the crematory's modified model, in which the primary burner angle is 25^o downward and the air nozzle's angle is 30^o and 30^o along the z-axis and y-axis respectively, can reach an average temperature of around 1,500 K, which is enough to eliminate pollutants released after corpse combustion. Furthermore, the modified model could achieve the highest effectiveness for things such as gas flow and blending between fuel gas and air. For NO formation, it was found that the rate of NO formation decreases when both primary and secondary chambers are operated, compare to that in only primary chamber operation. Although these simulation results are different from an actual cremation due to the fact that a corpse's moisture evaporation and disintegration were not considered, nevertheless, the results exhibit several benefits to the design and construction of high-efficiency double-chambered crematories using biomass-derived gas as fuel.

ACKNOWLEDGEMENT

The authors would like to acknowledge the Dean of the Faculty of Engineering, Chiang Mai University, the faculty's lecturers and staff members for all their assistance, Associate Professor Kulachate Pienthong (Ubon Rajathani University) and Mr.Thanadej Kantachote, Manager of J.E.N. Construction CO. LTD, for all of their valuable comments and suggestions.

REFERENCES

[1] S. Thavornun, *Study and research on crematory for energy saving*, Research's report, Energy Policy and Planning Office, Ministry of Energy of Thailand, 2007.

[2] N. Doungsupa et.al., Simulation of combustion in ceramic fiber kiln using computational fluid dynamics, *Proceeding of 11th Tri-University and Symposium Role of Asia in the Would*, 2004, 192-195.

[3] N. Vorayos, *Numerical modeling of air flow inside tobacco curing barn*, Research's report, Department of Mechanical Engineering, Faculty of Engineering, Chiang Mai University, 2002.

[4] S.V. Patanka, *Numerical heat transfer and fluid flow* (Hemisphere Publishing Corporation, NY: Taylor & Francis, 1980).

[5] Y. Achawangkul et.al., Biomass gasification utilization for double chambers crematory, *Proceeding of 2013 International Conference on Alternative Energy in Developing Countries and Emerging Economies (2013 AEDCEE)*, Bangkok, Thailand.